

A model for controlling the resting membrane potential of cells using nanoparticles

Shayok Mukhopadhyay, Fumin Zhang, Emilie Warren and Christine Payne

Abstract—This paper presents a novel dynamical system model for the resting membrane potential of cells. The novelty of this work is that the model allows parameters related to permeabilities of ion channels to be controlled so the resting membrane potential reaches a desired value. We are then able to explain the decreased polarity across the cell membrane when nanoparticles are introduced in the vicinity of a cell. The effect of varying these parameters on the resting membrane potential of a cell is investigated. The proposed model allows simulation of the behaviors of the resting membrane potential that matches experimental data.

I. INTRODUCTION

The transmembrane potential is the difference in electric potential between the interior and the exterior of biological cells. The transmembrane electrical potential of cells is of great importance in human health and disease [1]. This $-100mV$ to $-10mV$ gradient of electrical energy across the plasma membrane influences the transport of nutrients, ions, and water in and out of cells [1]. Different cell types have different characteristic membrane potentials [2]. Important for human disease, cancer cells are depolarized relative to healthy cells from the same tissue with resting membrane potentials closer to $0mV$. If the transmembrane potential can be controlled, it may be possible to influence the behavior of a cell so that certain diseases may be cured.

Multiple models have been generated to describe the transmembrane potential. Best known is the Hodgkin-Huxley model for the membrane current in active nerve cells [3]. Transport through the cell membrane has also been studied in [4]. Homeostasis is a property of a system in which certain variables are regulated to maintain a relatively stable internal environment. The work in [5] focuses on the dynamics of homeostasis and examines how long it takes to reach the equilibrium state if homeostasis is perturbed by a small amount. Steady-state analysis for modeling homeostasis for epithelial cells is presented in [6]. A system of differential equations linking transmembrane potential, ionic concentrations and cell volume of eukaryotic cells is examined in [7]. Although the model in [7] is useful, it is complex and it does

not explicitly deal with controlling the resting membrane potential. One of our motivations is to derive a simpler model which allows control of the transmembrane potential.

Lacking from previous models of transmembrane potential are parameters that allow control of the membrane potential. This paper presents a dynamic model that explicitly reveals the connections between the values of the tunable parameters and the values of the resting membrane potential. In addition, we show that our model is a nonlinear system that is stable over a large range of values for the parameters. Such a model can be used to simulate how the transmembrane potential reacts to the introduction of an ion species or how nanoparticles might be used to block specific ion channels to tune membrane potential [8]. The ability to target and modify cells by manipulating membrane potential has important implications for cancer detection and treatment. Biological processes like transmembrane potential, or genetic memory circuits, may have nonlinear dynamics [9]. Studying the stability properties of a nonlinear system may help understand the corresponding biological process [10], this is a motivation for us. Literature exists on simulating nonlinear biological processes [11]. Using nonlinear equivalent circuit models may make the dynamics of biological processes more accessible for control-oriented analysis. Thus inspired, we develop a simple nonlinear dynamic model of the transmembrane potential of a cell, the simplicity may aid a nonlinear equivalent circuit representation of our model in the future.

The main contribution of this work is a simple dynamic model that allows the control of cellular resting membrane potential by regulating the permeability of transmembrane channels. Unlike some existing approaches in the literature, our model also displays stability in addition to giving predictable values of the resting membrane potential. We argue that stability is a merit for any such model. We also show that one of the existing models in literature [12] produces a dynamic model with unstable equilibrium points, and this does not match physical observations. Our experimental efforts also show that the model successfully predicts the depolarization of cells when nanoparticles are introduced into the vicinity of cells. The dynamic model presented here can also be used to study the transient behavior of the transmembrane potential.

This paper is organized as follows. We motivate this work by providing experimentally observed results in section II. Background on cellular models is provided in section III. Our proposed model for controlling the transmembrane potential is presented in section IV. An analysis of the stability of the equilibrium points of this model is presented in section V.

This research was partially supported by the ONR grants N00014-08-1-1007, N00014-09-1-1074, and N00014-10-10712 (YIP), and NSF grants ECCS-0841195 (CAREER), CNS-0931576, and ECCS-1056253. Shayok Mukhopadhyay is with the Department of Electrical Engineering, American University of Sharjah, PO Box 26666, Sharjah, UAE. Fumin Zhang is with the School of Electrical and Computer Engineering, Georgia Institute of Technology, Atlanta, GA 30322, USA. Emilie Warren and Christine Payne are with the School of Chemistry and Biochemistry, College of Sciences, Georgia Institute of Technology, Atlanta, GA 30322, USA. Emails: smukhopadhyay@aus.edu, fumin@gatech.edu, ewarren6@gmail.com, christine.payne@chemistry.gatech.edu

Results of simulations and comparison of simulation results with experiments are presented in section VI. Conclusions and ideas for future work are presented in section VII.

II. MOTIVATION

Figures 1 and 2 show the results of binding nanoparticles to the membrane of CHO (Chinese Hamster Ovary) cells. The nuclei of the cells are stained with DAPI (4, 6-diamidino-2-phenylindole) and fluoresce blue, while the cytosol (intracellular fluid) are stained with DiBAC₄(3) (bis-(1,3-dibutylbarbituric acid) trimethamine oxonol) and fluoresce green. The properties of DiBAC₄(3) are such that, with increased depolarization, the dye diffuses into the cell to a greater extent than it does at the cell's resting state. Therefore, the cells exhibit an increase in DiBAC₄(3) fluorescence in response to an increased depolarization [13]. Figure 1 shows the control condition, before nanoparticles are introduced to the CHO cells. The cytosol of the cells do show a slight green fluorescence from DiBAC₄(3), due to the fact that some dye will enter into the cells even at their resting state, where the potential has some initial negative value in millivolts.

Figure 2 shows the same cells, but with the introduction

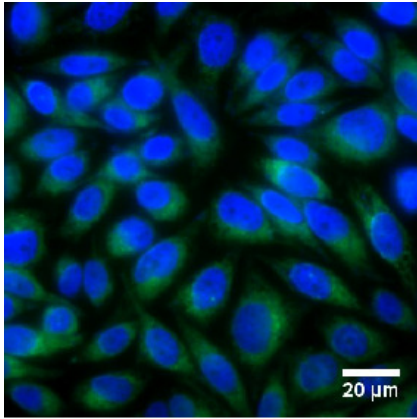


Fig. 1. Fluorescence microscopy image of CHO cells. Nuclei are stained with DAPI (blue) and the cytosol is stained with DiBAC₄(3) (green).

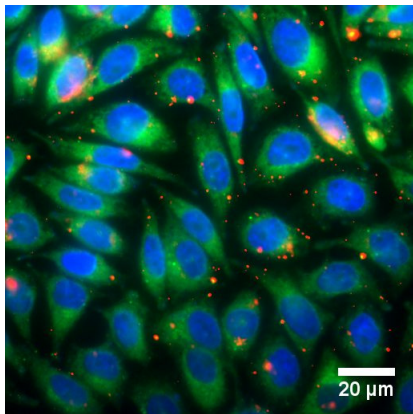


Fig. 2. Fluorescence microscopy image of 60nm amine-modified polystyrene nanoparticles (red), bound to the membrane of CHO cells.

of 60nm, amine-modified polystyrene nanoparticles. These red-fluorescent nanoparticles are introduced to the cells at conditions such that the particles bind to the outside of the plasma membrane. From Fig. 2 it is observed that the addition of nanoparticles has led to an increase in DiBAC₄(3) fluorescence. This increase in DiBAC₄(3) fluorescence after the introduction of nanoparticles indicates an increased depolarization of the cell. To define further, an increase in depolarization means that the transmembrane potential increases and approaches zero.

Motivated by the above observations, the aim of this paper is a simple dynamical model which allows certain parameters to be controlled, to allow us to mimic the effect of introducing nanoparticles (or any ion species) to make the transmembrane potential approach zero (or some other desired value). In the following section we provide some background information about modeling biological cells and then we propose our own model.

III. BACKGROUND

The work in [12] provides an accessible treatment to the problem of modeling the resting transmembrane potential of a cell. The following information from [12] forms the basis for the work in this paper.

A simple model showing a cell under standard conditions is shown in Fig. 3. The cell membrane (boundary) contains channels to mediate the passive movement of three types of ions i.e. Cl (chlorine), Na (sodium), and K (potassium). These channels are gaps in the cell membrane that allow the passage of molecules between cells. The fluid contained inside a cell is known as the cytosol. The permeability of the resting cell is $P_K = 1.0$, $P_{Na} = 0.02$, and $P_{Cl} = 2.0$ (in arbitrary units). As shown in Fig. 3, the resting potential of the cell is $V_{mr} = -80mV$, and the resting volume is 1.0 (arbitrary units). All ion concentrations are specified in mM (millimoles). The internal concentration of $[Cl^-]$ ions is only $7mM$. This makes room for internally accumulated substances ($[Subs^-]$) at a concentration of $143mM$. Note that the sum of the concentrations of ions and substances inside the cell in Fig. 3 equals the sum of the ion concentrations outside it, i.e. the cell shown is in homeostasis with internal conditions balanced relative to the outside.

The currents corresponding to the movement of a particular ion species through the channels shown in Fig. 3 are given by the following equations [12, Equation (3b)]. Consider the following.

$$\psi(t) = \frac{F}{RT} V_m(t) \quad (1)$$

$$I_K(\psi(t)) = P_K F z_K \left([K^+]_i - [K^+]_o e^{\psi(t)} \right) \quad (2)$$

$$I_{Na}(\psi(t)) = P_{Na} F z_{Na} \left([Na^+]_i - [Na^+]_o e^{\psi(t)} \right) \quad (3)$$

$$I_{Cl}(\psi(t)) = P_{Cl} F z_{Cl} \left([Cl^-]_o - [Cl^-]_i e^{\psi(t)} \right). \quad (4)$$

Here $P_X(cm/s)$ is the product of the number of pores per unit length of the cell membrane (cm^2) times the permeability $\rho_X (cm^3 pore^{-1} s^{-1})$ of a single pore. The subscript X

can be replaced with K, Na or Cl to reflect permeabilities to specific ions. F ($C\text{mol}^{-1}$) is Faraday's constant. The dimensionless quantities $z_K = z_{\text{Na}} = z_{\text{Cl}} = 1$, represent the number of valence electrons (unity for all ions considered here). All the internal, and external ion concentrations ($[\text{K}^+]_i$, $[\text{Na}^+]_i$, $[\text{Cl}^-]_i$, $[\text{K}^+]_o$, $[\text{Na}^+]_o$, $[\text{Cl}^-]_o$) belong to the interval $[0, \infty)$. The symbols R, T represent the gas constant and the absolute temperature in degrees Kelvin respectively, and the dimensionless quantity $\psi(t) \in \mathbb{R}$ is the ratio of the potential $V_m(t)F$ to the random thermal energy RT .

In addition to containing passive channels, the cell membrane also contains active units that transport ions/molecules inside/outside a cell. Figure 3 shows an ion pump. This pump exports three Na^+ ions and imports two K^+ ions in every cycle of its operation. Such active pumps may be driven by an energy source like ATP (adenosine triphosphate) molecules. The following equations govern the flux of Na^+ and K^+ ions through the ATP driven ion pump (shown by the empty circle in Fig. 3).

$$\Gamma_{\text{Na}^+}(t) = \frac{2.17[\text{ATP}]}{\left(1 + \frac{[\text{Na}^+]_c}{[\text{Na}^+]_i}\right)^3} \quad (5)$$

$$\Gamma_{\text{K}^+}(t) = \frac{-1}{\beta} \Gamma_{\text{Na}^+}(t), \quad (6)$$

where $\Gamma_{\text{Na}^+}, \Gamma_{\text{K}^+} \in \mathbb{R}$ represent the fluxes of Na^+ and K^+ ions respectively through the ion pump. The constant $\beta \in [0, \infty)$ represents the pump ratio (known). The quantity $[\text{Na}^+]_c \in [0, \infty)$ represents the concentration for half-maximal occupation of a Na^+ binding site on the pump. For details regarding active ion pumps, readers are encouraged to refer to [14]. Note that $[\text{ATP}] \in [0, \infty)$ is dependent on time, hence the L.H.S. in (5) and (6) is time-varying. The pump current [12] $I_{\text{pump}}(t) \in \mathbb{R}$ can now be obtained as

$$I_{\text{pump}}(t) = \left(\Gamma_{\text{Na}^+}(t) + \Gamma_{\text{K}^+}(t)\right) F. \quad (7)$$

The following relationship modeling the effect of the pump current, and the ion currents on the membrane voltage V_m can now be written as

$$I_{\text{Na}}(\psi(t)) + I_{\text{K}}(\psi(t)) + I_{\text{Cl}}(\psi(t)) + I_{\text{pump}}(t) = C_m \dot{V}_m(t). \quad (8)$$

In (8) $C_m \in (0, \infty)$ is the transmembrane capacitance. There are charged ions lining the inside and the outside of the cell membrane as seen in Fig. 3. The interior and the exterior of a biological cell can therefore be viewed as two electrically conducting regions, separated by a thin layer of insulating material (the cell membrane). For this reason, the presence of the cell membrane is modeled as the membrane capacitance C_m in (8). Equation (8) provides a basic equation that needs to be satisfied by the various currents through the membrane and the transmembrane potential. Solutions for V_m may not necessarily be trivial.

IV. THE PROPOSED MODEL

We desire to be able to alter the value of V_m by changing the flux through each channel using nanoparticles.

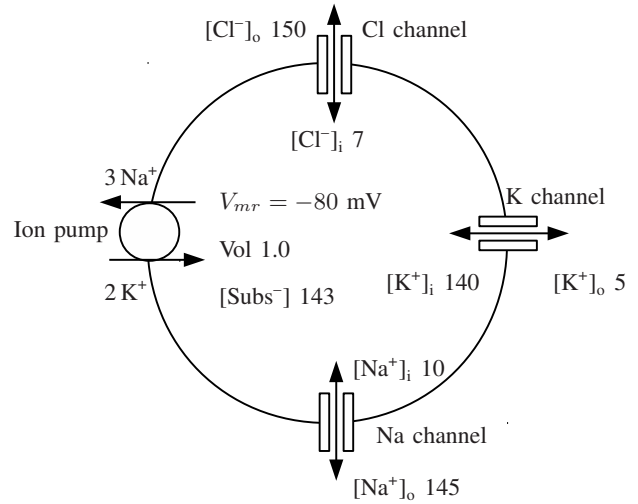


Fig. 3. A model showing the normal condition of a cell [12].

Now consider the parameters $\alpha_1, \alpha_2, \alpha_3 \in [0, \infty)$, and the parameter $k \in (0, \infty)$ defined as $\alpha_1 = P_K F z_K$, $\alpha_2 = P_{\text{Na}} F z_{\text{Na}}$, $\alpha_3 = P_{\text{Cl}} F z_{\text{Cl}}$, and $k = \frac{F}{RT}$. Note that Faraday's constant F , the gas constant R are positive. The normal operating temperature of a cell is expected to be bounded and significantly above absolute zero, hence $T \in (0, \infty)$. Therefore we have that the constant $k > 0$. Equations (2)-(4) can now be re-written as follows,

$$I_{\text{K}}(V_m(t)) = \alpha_1 [\text{K}^+]_i - \alpha_1 [\text{K}^+]_o e^{kV_m(t)} \quad (9)$$

$$I_{\text{Na}}(V_m(t)) = \alpha_2 [\text{Na}^+]_i - \alpha_2 [\text{Na}^+]_o e^{kV_m(t)} \quad (10)$$

$$I_{\text{Cl}}(V_m(t)) = \alpha_3 [\text{Cl}^-]_o - \alpha_3 [\text{Cl}^-]_i e^{kV_m(t)}. \quad (11)$$

Using equations (9)-(11), equation (8) can be re-written as follows.

$$\begin{aligned} \dot{V}_m(t) = & \frac{1}{C_m} (\alpha_1 [\text{K}^+]_i + \alpha_2 [\text{Na}^+]_i + \alpha_3 [\text{Cl}^-]_o) \\ & - \frac{e^{kV_m(t)}}{C_m} (\alpha_1 [\text{K}^+]_o + \alpha_2 [\text{Na}^+]_o + \alpha_3 [\text{Cl}^-]_i) \\ & + \frac{1}{C_m} I_{\text{pump}}(t) \end{aligned} \quad (12)$$

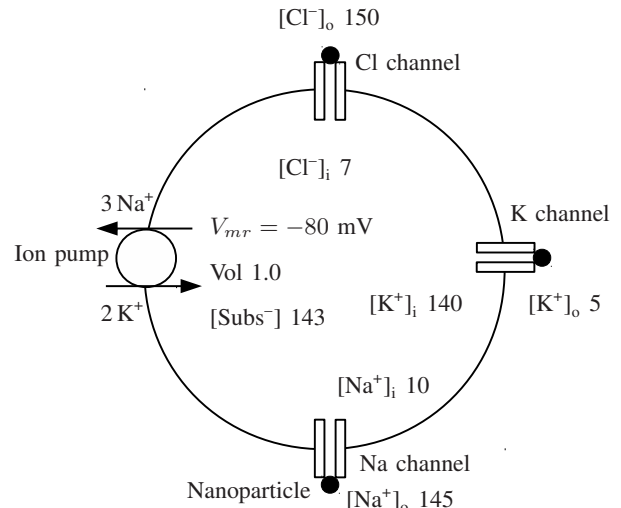


Fig. 4. A model showing channels of a cell blocked using nanoparticles.

The concentrations of ions outside a cell i.e. $[K^+]_o$, $[Cl^-]_o$, and $[Na^+]_o$, can be regarded as a constant or slowly varying compared to the dynamic change of the transmembrane potential [14]. This is because the environment external to a cell can be considered a chemical reservoir with constant concentrations. Also, to maintain normal operating conditions within a cell, every particular type of cell maintains the concentrations of ions inside a cell i.e. $[K^+]_i$, $[Cl^-]_i$, and $[Na^+]_i$, at constant values [14]. The channel currents arise due to the movement of ions to maintain such a required steady potential difference. The ion pump current is also maintained at a relatively steady value [14], because any transient disturbance in the pump current magnitude will most likely upset the chemical concentrations within a cell, i.e. disrupt the required operating conditions. Based on the above discussion, the following simplifications are made,

$$a = \frac{1}{C_m} (\alpha_1 [K^+]_i + \alpha_2 [Na^+]_i + \alpha_3 [Cl^-]_o) \quad (13)$$

$$b = \frac{1}{C_m} (\alpha_1 [K^+]_o + \alpha_2 [Na^+]_o + \alpha_3 [Cl^-]_i) \quad (14)$$

$$c = \frac{1}{C_m} \quad (15)$$

$$I_{pump}(t) = d, \quad (16)$$

where the parameters $a, b \geq 0$, and $c, d > 0$. Note that the pump current and the ion concentrations have constant values for a cell in normal operating conditions. In (13)-(15) the quantity C_m , which represents the transmembrane capacitance of a cell, is already known. The constants α_1, α_2 and α_3 can be chosen to have particular values. In general the values of the constants α_1, α_2 and α_3 can be altered by the introduction of some ion species in/around a cell. In this work, it is assumed that the introduction of nanoparticles is used to make the constants α_1, α_2 and α_3 have desired values. From (13) and (14) it is seen that a, b depend on the values of α_1, α_2 and α_3 . Therefore changing α_1, α_2 and α_3 by the introduction of nanoparticles can allow us to change the parameters a or b .

Using (13)-(16), the model in (12) can be re-written as,

$$\dot{V}_m(t) = a - be^{kV_m(t)} + cd, \quad \text{where } k, c, d > 0, \text{ and } a, b \geq 0. \quad (17)$$

Now let the state variable $z(t) = e^{kV_m(t)}$, taking the time derivative of z and using (17) we get $\dot{z}(t) = ke^{kV_m(t)} \dot{V}_m(t)$, which gives the following system equation.

$$\dot{z} = kz(a - bz + cd) \quad (18)$$

V. STABILITY ANALYSIS

From (18) it can be seen that $\dot{z} = 0$ when z assumes the following two values,

$$z_{01} = 0, \quad \text{and} \quad (19)$$

$$z_{02} = \frac{a + cd}{b}, \quad (20)$$

representing the two equilibrium points for the system in (18). From (18) and (20) we get,

$$\dot{z} = -kbz(z - z_{02}). \quad (21)$$

The equilibrium point $z_{01} = 0$ for (18) corresponds to $V_{mr} = -\infty$. This equilibrium point is not practically useful because a resting membrane potential of $V_{mr} = -\infty$ is not normally observed [2]. Therefore we use the restriction $z \neq 0$. Since $z = e^{kV_m}$, this implies $z > 0$ and therefore get the following stable system.

$$\dot{z} = -kbz(z - z_{02}), \quad \text{where } k, b, z > 0 \quad (22)$$

Stability of (22) can be easily verified by linearization if required, or considering the candidate Lyapunov function [15] $V = \frac{1}{2}(z - z_{02})^2$, the time derivative of which gives $\dot{V} = -kbz(z - z_{02})^2 < 0$. For a normal cell the ion channels are not completely blocked i.e. the condition $b > 0$ is valid for a cell in normal operating conditions. Further, from (20) and the definition of z , the resting membrane potential corresponding to the stable equilibrium z_{02} is given by

$$V_{mr} = \frac{1}{k} \ln \left(\frac{a + cd}{b} \right). \quad (23)$$

The pump current d is not available for control, and a/b has a constant value. But as b tends to infinity, the term cd/b in (23) vanishes. Therefore, it is possible to alter the resting membrane potential by changing b . This may be achieved by increasing or lowering ion channel permeabilities by using an ion species. Using nanoparticles will block ion channels in the cell membrane, thus reducing the permeability values α_1, α_2 and α_3 and thereby reducing the value of the parameter b . For certain values of a/b , the introduction of nanoparticles is expected to make z_{02} approach unity, and V_{mr} approach 0.

Here it must be noted that the using [12, Equation (3b)] and not [12, Equation (3a)] results in the stable system given in (22). Using [12, Equation (3a)] results in a model with no stable equilibrium points. This does not agree with physical observations because the transmembrane potential stabilizes to the resting membrane potential, therefore we have used [12, Equation (3b)]. Further, if an unstable system model based on [12, Equation (3a)] was used, then it would not be possible to regulate the resting membrane potential V_{mr} by changing the parameter b .

The effects of introducing nanoparticles on the resting membrane potential is investigated by using simulations and also by performing actual experiments. The results of the simulations and experiments are compared in the next section.

VI. SIMULATIONS AND EXPERIMENTS

Here we present the results based on the theoretical discussion in the previous sections, and also compare them with actual results of using nanoparticles to alter the resting membrane potential of CHO cells. Although a and b are defined in (13) and (14) to depend on the individual channel permeabilities α_1, α_2 and α_3 , expecting such fine grained control may be impractical. This is because a cell has many channels, and it may be very involved (if not impossible) to quantify the effect of introducing a particular type of nanoparticle on a specific ion channel. Therefore for

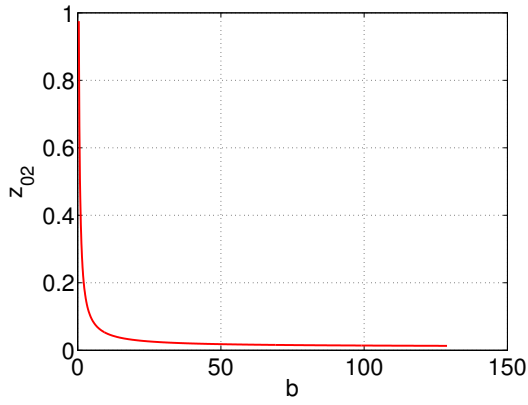


Fig. 5. A plot showing z_{02} vs. b .

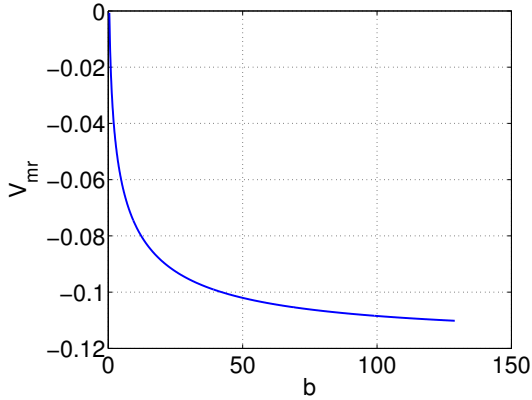


Fig. 6. A plot showing V_{mr} vs. b .

simulations, (and to match the experimental situation) it is feasible to redefine a, b to model the overall effect of the ion concentrations inside/outside a cell. For this purpose, let us simplify (13) and (14) to the following,

$$a = \gamma_1 ([K^+]_i + [Na^+]_i + [Cl^-]_o) \quad (24)$$

$$b = \gamma_2 ([K^+]_o + [Na^+]_o + [Cl^-]_i) \quad (25)$$

where $\gamma_1(\cdot) = 0.01\gamma_2(\cdot)$ for our simulations. The specific relation $\gamma_1(\cdot) = 0.01\gamma_2(\cdot)$ is chosen so the simulation results produce values for the resting membrane potential which lie in the practically observed range.

A. Simulation results

From (24), (25) we have $a/b = 0.01$. For the simulations we set the capacitance $C_m = 37pF$ (picofarads), temperature $T = 22^\circ C$, $R = 8.314JK^{-1}mol^{-1}$, $F = 96485Cmol^{-1}$ and the cell current $d = 15pA$ (picoamperes). Note that the values for the capacitance and current have been chosen in accordance with values observed in [16]. The following plots are obtained for the state z and the resting membrane potential V_{mr} calculated using (23), by smoothly varying b in the interval $[0.42, 129]$. Figure 5 shows how the equilibrium point z_{02} varies as b is varied between 0.42 and 129. It is observed from Fig. 5 that as the positive number b is

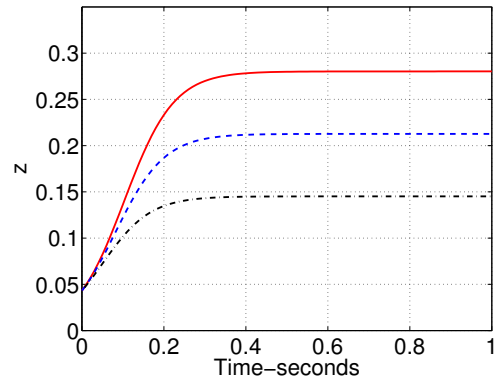


Fig. 7. A plot showing trajectories $z(t)$ of the system in (18) for increasing values of b . Red-solid curve corresponds to $b = 1.5$, blue-dashed curve corresponds to $b = 2$, and black dash-dotted curve corresponds to $b = 3$.

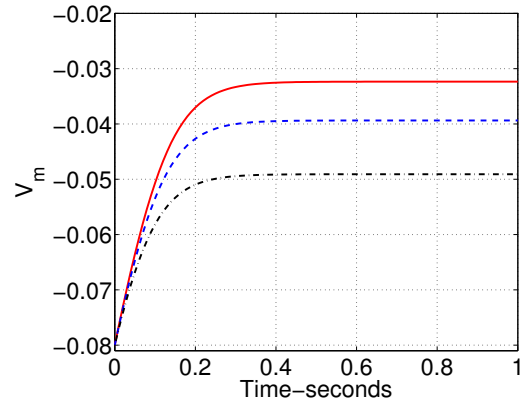


Fig. 8. A plot showing the transmembrane potential $V_m(t)$ for increasing values of b . Red-solid curve corresponds to $b = 1.5$, blue-dashed curve corresponds to $b = 2$, and black dash-dotted curve corresponds to $b = 3$.

decreased, z_{02} approaches unity. And as b is increased z_{02} approaches $\frac{a}{b} = 0.01$ in this case.

Figure 6 shows how the resting membrane potential V_{mr} varies as b is varied between 0.42 and 129. Recall that $z = e^{kV_m}$, this implies that as z approaches $\frac{a}{b} = 0.01$ corresponding to an increase in b then V_{mr} must tend to some negative number. Such behavior is verified from Fig. 6 where the resting membrane potential V_{mr} is seen to approach $-0.11V$ as b is increased towards 129. Similarly, a decrease in b causes z to increase towards unity, which causes V_{mr} to approach zero. This behavior is also clearly observed in Fig. 6 where V_{mr} is seen to approach zero as b approaches 0.42. Also note that lower values for b correspond to lower permeability values for the ion channels and higher values for b correspond to a situation with ion channels having higher permeability, as per the definitions in (24) and (25).

The plots in figures 7 and 8 show how the state z of the system in (18), and therefore the transmembrane potential $V_m(t)$ stabilizes to different resting membrane potentials V_{mr} corresponding to a change in b . In both Fig. 7 and Fig. 8 the red-solid curve corresponds to $b = 1.5$, the blue-dashed curve corresponds to $b = 2$, and black dash-dotted curve corresponds to $b = 3$. An initial value of $-80mV$

corresponding to the normal operating conditions of a cell is assumed to be the initial condition for V_m , therefore all the curves in Fig. 7 and Fig. 8 appear to begin from the same initial point. As observed in Fig. 5 and Fig. 6, an increase in b results in a decrease in z towards zero, and the resting membrane potential V_{mr} decreases towards further negative values. This behavior is clearly seen in figures 7 and 8 as well. As b increases from 1.5 to 3, the trajectories for $z(t)$ in Fig. 7 stabilize to values closer to zero. Similarly in Fig. 8 it is seen that as b increases from 1.5 to 3, the transmembrane potential stabilizes to progressively more negative values. We now proceed to verify if these observations are confirmed by experimental results.

B. Comparison with experimental results

As mentioned in section II, from Fig. 2 it is observed that the addition of nanoparticles has led to an increase in DiBAC₄(3) fluorescence. An increase in DiBAC₄(3) fluorescence indicates an increased depolarization of the cell. An increase in depolarization implies that the transmembrane potential increases and approaches zero. From the discussion in section IV-B, this implies that introducing the nanoparticles may have actually decreased the permeability of certain channels in CHO cells so that the resting membrane potential approaches zero (see Fig. 6, a decrease in b causes V_{mr} to approach zero. Since b depends on the permeability of ion channels (the ion concentrations and the transmembrane capacitance remaining constant), a decrease in b implies that the introduction of nanoparticles results in a decrease in ion channel permeabilities, which causes the membrane potential to approach zero. Therefore our simulations agree with the experimental observations.

VII. CONCLUSIONS AND FUTURE WORK

A. Conclusions

A simple dynamical model is presented for the transmembrane potential of cells. This model allows the control of the resting membrane potential by manipulating physiological parameters. It is shown that standard cellular conditions correspond to one stable equilibrium of the model. Based on the theoretical developments and the results from simulations and experiments, we can conclude that introducing nanoparticles can alter the transmembrane potential. The simulation results based on the model developed in this paper agree with the experimental results suggesting that the introduction of nanoparticles reduces ion channel permeability, making the resting membrane potential approach zero. The plot shown in Fig. 6, can be quickly generated for different types of cells in order to figure out if a particular resting membrane potential is achievable, and what approximate value for the term b may be required. This model can be used prior to experiments to achieve the desired resting membrane potential.

B. Future work

In the future, methods for implementing real-time state-feedback control within a cell may become available, this can help control the transients of the resting membrane potential

in response to chemical imbalances. The ability to predict if the transmembrane potential of a cell can reach a target value may help in the use of membrane potentials as a target for cancer treatment.

REFERENCES

- [1] S. Wright, "Generation of resting membrane potential," *Advances in Physiology Education*, vol. 28, no. 1-4, pp. 139–142, 2004.
- [2] M. Yang and W. Brackenbury, "Membrane potential and cancer progression," *Frontiers in Physiology*, vol. 4, pp. 185:1–185:10, 2013.
- [3] A. Hodgkin and A. Huxley, "A quantitative description of membrane current and its application to conduction and excitation in nerve," *The Journal of Physiology*, vol. 117, pp. 500–544, 1952.
- [4] X. Zhang, K. Shedden, and G. Rosania, "A cell based molecular transport simulator for pharmacokinetic prediction and cheminformatic exploration," *Molecular Pharmaceutics*, vol. 3, no. 6, pp. 704–716, 2006.
- [5] A. Weinstein, "Dynamics of cellular homeostasis: Recovery time for a perturbation from equilibrium," *Bulletin of Mathematical Biology*, vol. 59, no. 3, pp. 451–481, 1997.
- [6] A. Weinstein, "Modeling epithelial cell homeostasis: Steady-state analysis," *Bulletin of Mathematical Biology*, vol. 61, pp. 1065–1091, 1999.
- [7] C. Poinard, A. Silve, F. Campion, L. Mir, O. Saut, and L. Schwartz, "Ion fluxes, transmembrane potential, and osmotic stabilization: A new dynamic electrophysiological model for eukaryotic cells," *European Biophysics Journal*, vol. 40, pp. 235–246, 2011.
- [8] E. H. Shin, Y. Li, U. Kumar, H. V. Sureka, X. Zhang, and C. K. Payne, "Membrane potential mediates the cellular binding of nanoparticles," *Nanoscale*, vol. 5, pp. 5879–5886, 2013.
- [9] Y. Zhang and P. Li, "Gene-regulatory memories: Electrical-equivalent modeling, simulation and parameter identification," in *IEEE/ACM International Conference on Computer-Aided Design - Digest of Technical Papers*, 2009, pp. 491–496.
- [10] Y. Zhang, P. Li, and G. M. Huang, "Quantifying dynamic stability of genetic memory circuits," *IEEE/ACM Transactions on Computational Biology and Bioinformatics*, vol. 9, pp. 871–884, 2012.
- [11] M. E. Jackson and J. W. Gnad, "Numerical simulation of nonlinear feedback model of saccade generation circuit implemented in the LabView graphical programming language," *Journal of Neuroscience Methods*, vol. 87, pp. 137–145, 1999.
- [12] C. Armstrong, "The Na/K pump, Cl ion, and osmotic stabilization of cells," in *Proceedings of the National Academy of Sciences of the United States of America*, vol. 100, no. 10, 2003, pp. 6257–6262.
- [13] T. Klapperstück, D. Glanz, M. Klapperstück, and J. Wohlrab, "Methodological aspects of measuring absolute values of membrane potential in human cells by flow cytometry," *Cytometry, Part A: Journal of the International Society for Advancement of Cytometry*, vol. 75, pp. 593–608, 2009.
- [14] B. Alberts, A. Johnson, J. Lewis, M. Raff, K. Roberts, and P. Walter, *Molecular Biology of the Cell*, 5th ed. Garland Science, 2007.
- [15] H. K. Khalil, *Nonlinear Systems*, 3rd ed. Prentice Hall, 2002.
- [16] R. Dipolo and A. Marty, "Measurement of Na-K pump current in acinar cells of rat Lacrimial glands," *Journal of Biophysics*, vol. 55, pp. 571–574, 1989.